Anisotropic thermal-lens effect in ferroelectric $Ba_2NaNb_5O_{15}$ at T_c

J. F. Scott, Shou-Jong Sheih, Karen R. Furer,* and Noel A. Clark
Department of Physics, University of Colorado, Boulder, Colorado 80309-0390

W. F. Oliver and S. A. Lee†
Department of Physics, Arizona State University, Tempe, Arizona 85287

(Received 15 May 1989; revised manuscript received 28 September 1989)

We have discovered a novel effect in barium sodium niobate at its Curie temperature $T_c = 853$ K, in which the large positive temperature derivative of the c-axis index of refraction associated with the ferroelectric phase transition, $dn_c/dT = +1.4\times10^{-3}$ K^{-1}, produces a convex (positive) thermal lens of typical focal length 3 cm. This is 30 times stronger than the isotropic thermal-lens effect found in fluids by Gordon *et al.*, and of the opposite sign. This effect potentially provides an accurate way of measuring dn/dT very near phase-transition temperatures, which may be of interest in studies of critical phenomena associated with structural phase transitions in solids. We find $2\beta = 0.58\pm0.05$ in the present study. Temporal effects are found to be in accord with the thermal-focusing theories for fluids and yield the thermal diffusivity at T_c accurately as well.

I. INTRODUCTION

The thermal focusing of laser beams in isotropic fluids has been understood in detail for more than twenty years as arising from thermal expansion;[1,2] the decreased density in the laser beam region produces a negative temperature derivative for the index of refraction of order $dn/dT = -1\times10^{-3}$ K^{-1} and a consequent concave (negative) lens of characteristic focal length $F = -1.0$ m. A physically different mechanism exists for even larger values of dn/dT in solids, which may be of either positive or negative sign: As shown in Fig. 1, $Ba_2NaNb_5O_{15}$ exemplifies the large changes in indices of refraction and birefringence associated with structural phase transitions in crystals. Here at T_c the value of $dn_c/dT = +1.4\times10^{-3}$ K^{-1}, about -2 times the value in typical fluids. The purpose of this paper is to show that this large temperature derivative can produce intense focusing near T_c. In addition to being a new optical effect of some intrinsic interest, careful measurements of such phenomena in crystals can provide very precise values of dn/dT near T_c; since birefringence measurements are particularly well suited to the study of critical phenomena associated with second-order phase transitions,[3] these new measurements may be of special utility in such investigations.

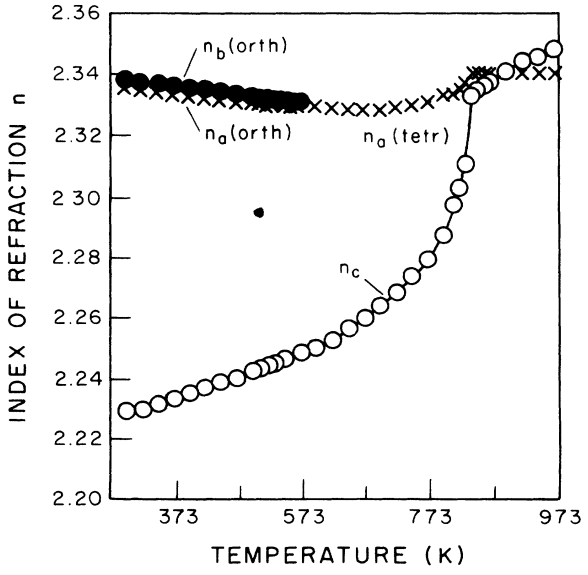

FIG. 1. Indices of refraction near T_c in $Ba_2NaNb_5O_{15}$ (Ref. 5).

II. THEORY

The theory of thermal focusing in fluids yields an expression for the time-dependent focal length $F(t)$ given by

$$F(t) = F_\infty(1 + t_c/2t)\ , \tag{1}$$

where

$$F_\infty = (\pi k_T n w_0^2)(0.24bPL dn/dT)^{-1} \tag{2}$$

with k_T as the thermal conductivity, n the index of refraction at the laser beam wavelength and the furnace temperature, b the fluid absorption coefficient, P the laser power inside the target fluid, dn/dT the temperature derivative of the index of refraction; and w_0 the laser beam waist radius.

F_∞ can also be measured geometrically from the angular divergence $+\theta$ of the beam emerging from the crystal. The simplest approximation gives

$$F_\infty = w_0/(1.6\theta)\ . \tag{3}$$

θ ranges from 1° to 11° or arc, depending upon power and temperature.[4] For fluids, F is typically -1.0 meters, cor-

responding to a weakly diverging lens. In our experiments we verified the positive sign of F by placing a convex lens in front of the $Ba_2NaNb_5O_{15}$ target. As it was moved closer to the target, the scattering angle θ increased. We interpret this as evidence that the thermal lens in $Ba_2NaNb_5O_{15}$ is focusing the laser beam through a focal point near the exit surface of the crystal. A similar positioning of a convex lens in front of a fluid exhibiting a thermal-lens effect decreases the angle θ.

Fortunately, for $Ba_2NaNb_5O_{15}$ all of the constants appearing in Eq. (2) are known. Near $T_c=855$ K the values are as follows: $n_c=2.33$,[5] $k_T=0.059$ W/cm K,[6] $b=0.257$ cm^{-1},[7] and $dn_c/dT=+1.4\times10^{-3}$ K^{-1}.[8] At maximum power, the parameters for our particular experiment are $P=1.0$ W; $L=0.3$ cm, and $w_0=0.45$ mm. These values give $F_\infty=3.0\pm0.3$ cm in Eq. (2) and $F_\infty\cong1.6\pm0.2$ cm in Eq. (3), which should be regarded as only rough agreement. The principal uncertainties are in absorption coefficient b, which varies with temperature (and by $\geq 50\%$ in different specimens at the same temperature) and the difficulty in applying Eq. (3) to a system with strong spherical aberration.

In addition, the time constant t_c appearing in Eq. (1) is not a freely adjustable parameter, but is given by[1]

$$t_c=\frac{w_0^2}{(4D_T)}\ , \tag{4}$$

where D_T is the thermal diffusivity and is a function of T. D_T is not known at T_C but equals[6] 0.02 cm^2/s at $\sim$400 K and should be somewhat larger at the temperatures of our experiments. Using our value of $w_0=0.045$ cm, Eq. (4) yields $t_c=25$ ms, in fairly good agreement with the values given in Fig. 2. The inclusion of spherical aberration, discussed next, causes t_c to depend upon power P.

The images of the refracted beams shown in Figs. 3(a) and 3(b) exhibit a strong ring pattern at the outer extremities of the patterns shown. This effect is due to spherical aberration, which becomes increasingly important at high power.[9] By adjusting the distance between the specimen and the screen, this ring diameter can be minimized for a

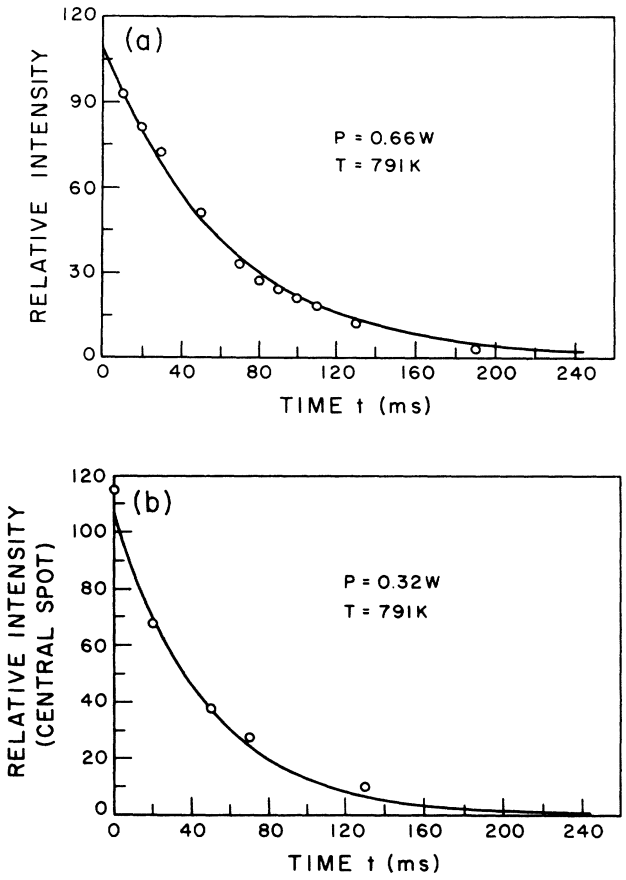

FIG. 2. (a) Intensity remaining in the central spot vs time t after laser is turned on, at a constant laser power of 0.6 W ($T=791$ K). The time constant t_c fitting this relaxation to steady state is 50 ms. Data are fitted to the aberrant lens model (Ref. 10). $I(t)=I_0\{(t+t_c)/[(1+\gamma P_0)t+T_c]\}^2$ in Fig. 2. A simple exponential fits the data approximately as well. At higher powers an oscillatory, nonexponential decay is observed; (b) at 0.33 W.

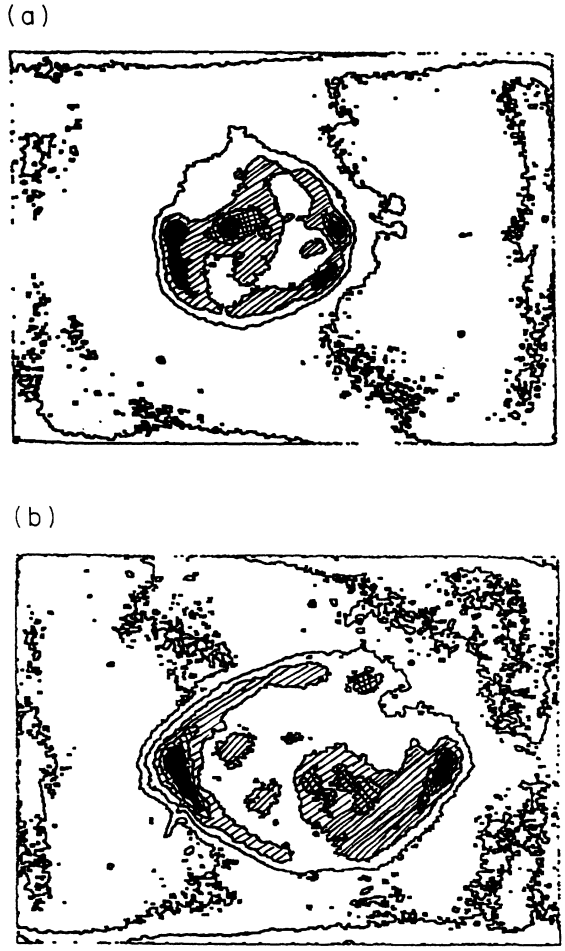

FIG. 3. Computerized contour maps of actual photographs of 514.5 nm Ar II laser light 1.0 m from a $Ba_2NaNb_5O_{15}$ target. Actual width is $\sim$2.0 cm (a) at 831 K; (b) at 833 K. Incident and scattered polarizations are both along the polar c axis. Power is $\sim$1 W.

given temperature and power, producing a "circle of least confusion." Our data show that spherical aberration is negligible for powers below 0.3 W, but becomes quite extreme (Fig. 3) for powers ~1 W. In liquids it has been found[2] that spherical aberration and convection set in at

$$P \geq \frac{1.6\lambda kT}{bLdn/dT} , \tag{5}$$

which for our experimental parameters gives 0.2 W, in good agreement with the onset of strong aberrations we observe above 0.3 W.

The basic theory of thermal focusing in fluids[1] has been modified to include such lens aberrations; Sheldon *et al.*[10] have considered an aberrant lens model that assumes the thermally induced phase shift is small, which modifies both the optimum position for placement of the specimen, and produces a change in both time constant and effective focal length of approximately a factor of 0.52. Qualitatively, the parabolic lens model gives a larger intensity change for a given power and a shorter response time t_c than does the aberrant lens model. Because the parameters occurring in the theories are imprecisely known for $Ba_2NaNb_5O_{15}$ (particularly the absorption coefficient b), we cannot discriminate between the models in detail; however, the factor of 0.52 ($=\tan^{-1}3^{-1/2}$) brings about somewhat better agreement between theory and experiment in the present case. In addition, the spherical aberration introduces a power dependence in t_c, which is otherwise absent [see Eq. (3)].

In addition to spherical aberration, there is also considerable astigmatism and curvature of field. This produces,

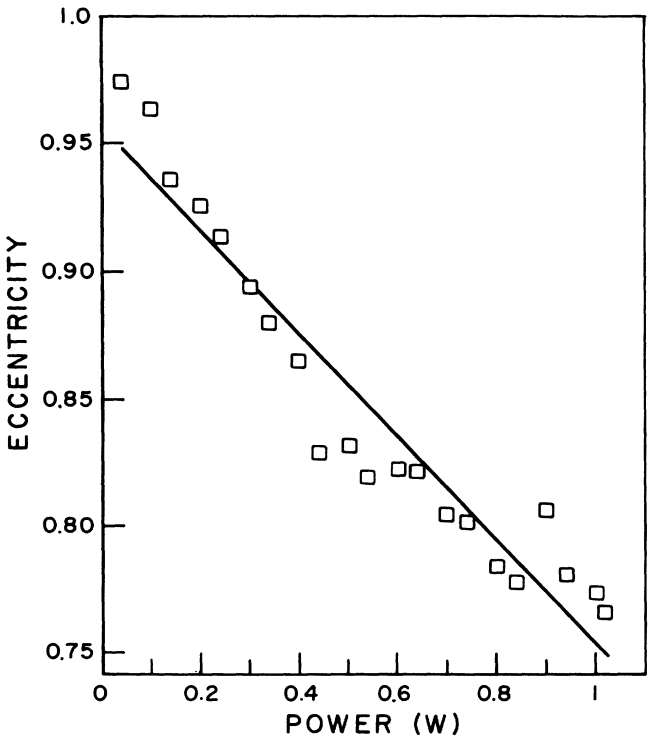

FIG. 4. Eccentricity of scattered ring vs power.

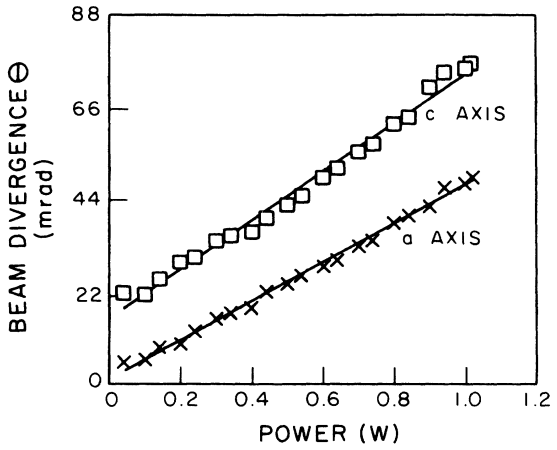

FIG. 5. Dependence of spot size vs laser power for c and a axes.

in general, an elliptical image [Fig. 3(b)], with semiaxes related to the coefficients in the aberration function.[9] In our experiments the eccentricity depends strongly upon power, as shown in Fig. 4. Usually it becomes more astigmatic with increasing power, as shown in Fig. 4; however, in some cases anisotropic power-independent aberrations along the c axis (even at $P \approx 0$) cause maximum eccentricity at lowest powers, with decreasing eccentricity as power is increased (Fig. 5).

Because of the strong spherical aberration and astigmatism (curvature of field), it is only a crude approximation to apply Eq. (3) to our data. The position at which a clear image is observed is not related in a simple way to the focal length; the "longitudinal spherical aberration" can be of order 1.0 m, much greater than the ~2-cm ring pattern ("transverse spherical abbrevation"). Therefore, the fact that F_∞ from Eqs. (2) and (3) agree only to a factor of 2 is not unreasonable. The ratio of longitudinal to transverse spherical aberration in our experiment is estimated[9] as

$$\frac{\Delta Z}{\Delta X} \cong \frac{Z}{X} , \tag{6}$$

where Z is the image distance, X the height of the (thermal) lens above the optic axis, ΔX the radius of the circle at least confusion due to the transverse spherical aberration, and ΔZ the shift in apparent focal length due to longitudinal spherical aberration. For our experiment $Z = 142$ cm, $X \cong 0.1$ cm, and $\Delta X \cong 1$ cm; hence ΔZ is estimated as ~0.1 m.

III. EXPERIMENT

A. Spatial patterns

The data described here were obtained with an argon-ion laser operating at powers of 0.1–1.0 W at 514.5 or 488.0 nm. The beam was weakly focused into an oriented crystal of barium sodium niobate positioned in a furnace whose temperature was controlled to about 0.1 K at temperature near $T_c = 853$ K. The effects reported following

were observed only for incident-beam polarization along the polar c axis; for other polarizations, no thermal focusing was observed. Figures 3(a) and 3(b) are photographs of the phenomena observed: They consist of elliptical rings of transmitted light of the same polarization as the incident beam, of varying eccentricities dependent upon power and temperature. The angular divergence of these beams from the crystal target was of order 1°–2° of arc and exhibited a strong time dependence; when the laser beam is turned on, the elliptical pattern will grow in angle from an initial value of zero (directly forward scattering) to a maximum of order 2°–10°, characterized by a rise time of 0.01–0.05 s, depending on power. Interruption of the beam shows that relaxation back to the original state is slower, typically requiring 5–6 s.

The theory described, and in particular Eq. (2), implies that the beam divergence along the c axis will vary as $(dn_c/dT)^{-1}$, which slowly increased as T_c is approached from below and then abruptly drops by approximately $\frac{1}{3}$ as T increases above T_c. T_c in our samples varied from 833 to 860 K. This prediction is in accord with the results of beam width θ shown for a single run at 0.4 W in Fig. 6 and for a larger data set in Fig. 7.

In Fig. 7(b) we show $\theta(T)$ for a single data set in which beam position, laser power, sample temperature, and convection currents in the oven were all carefully stabilized. If we assume that dn_c/dT is the only quantity in Eq. (2) that is singular as T approaches T_c, then $\theta(T)$ should vary from Eqs. (2) and (3) as $\epsilon^{2\beta-1}$, where ϵ is reduced temperature and β is the critical exponent associated with the coexistence curve. This assumes that the primary contribution to Δn_c is electro-optic, which varies as

$$\Delta n_c(T) = -n^3(g_{11}-g_{22})P_S^2(T)$$

where the coefficients g_{11} and g_{22} are known to vary slowly with temperature, and not due to elasto-optical coupling.[8] A plot in Fig. 7(c) of the raw data shown in Fig. 7(b) yields a value of $2\beta=0.58\pm0.05$, in good agreement with the mean-field prediction $\beta=\frac{1}{4}$ near tricritical points. It is known from earlier work[8] that T_c in $Ba_2NaNb_5O_{15}$ is very near a tricritical point.

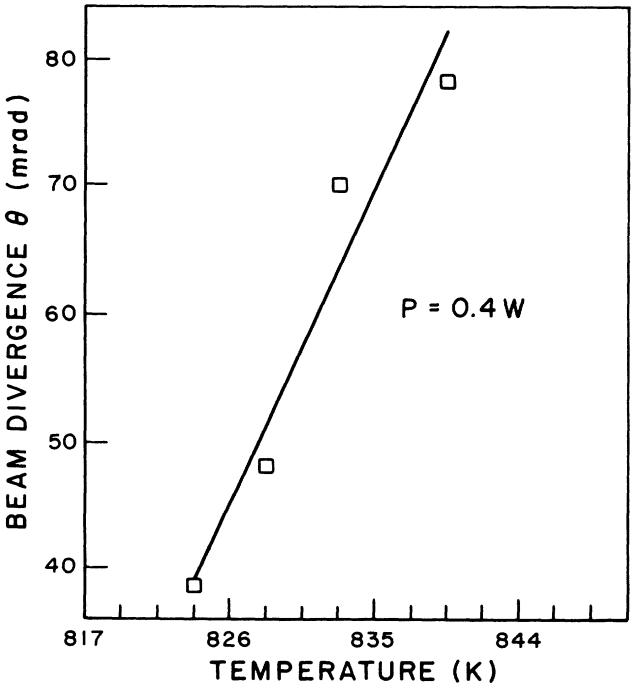

FIG. 6. Beam divergence θ vs T at $P=0.4$ W; single run.

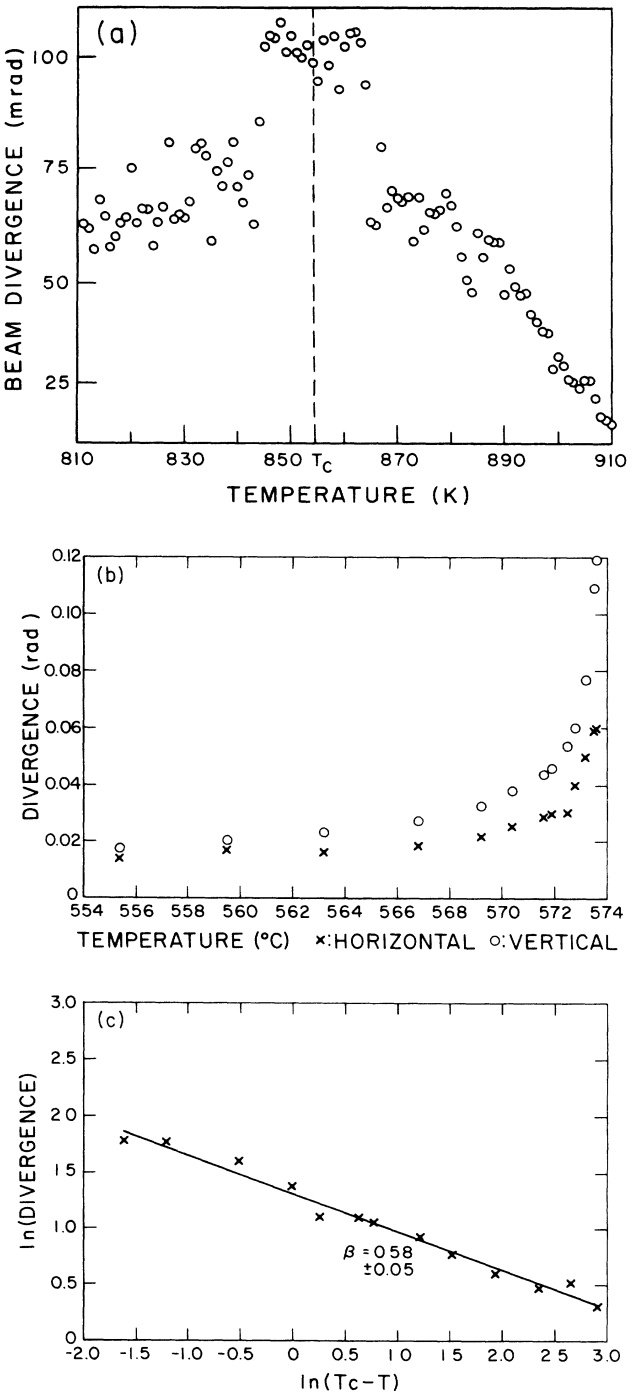

FIG. 7. Beam divergence θ vs T; multiple runs.

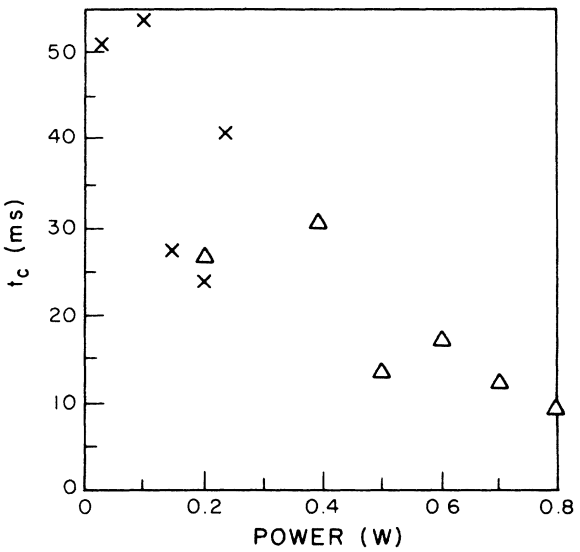

FIG. 8. t_c vs laser power P at $T=830$ K (△'s) and 791 K (×'s).

Note that if the experiment were also sensitive to singularities near T_c in the thermal conductivity K_T in Eq. (2), $\theta(T)$ would vary as $\epsilon^{2\beta-1-\nu+\gamma}=$const in mean-field theory. The data in Figs. 7(b) and 7(c) therefore imply that the experiment does not measure any divergence in K_T, which is in fact a notoriously difficult singularity to detect, due to convection effects, even in simple fluids.

B. Time dependence

We can test the time dependence of the focal length predicted in Eqs. (1) and (3) by measuring the decrease in intensity of the central transmitted spot of laser light with time t after the laser is turned on. Figure 2 shows that this decay is in accord with Eq. (1), with $t_c \cong 50-60$ ms at both $P=0.66$ and 0.32 W at $T=79$ K (well below T_c). The numerical value agrees with that predicted in Eq. (3) to within 50%, which is nearly the calculated uncertainty. This time constant actually depends upon power, as shown in Fig. 8, and upon temperature, becoming as fast as 12 ms very near T_c. The temperature dependence is in accord with Eq. (4), assuming that the thermal diffusivity D_T increases rapidly as $T \rightarrow T_c$. The power dependence observed experimentally is not accounted for in the simple theory summarized in Eq. (4) but presumably arises from increases in spherical aberration with increasing P.

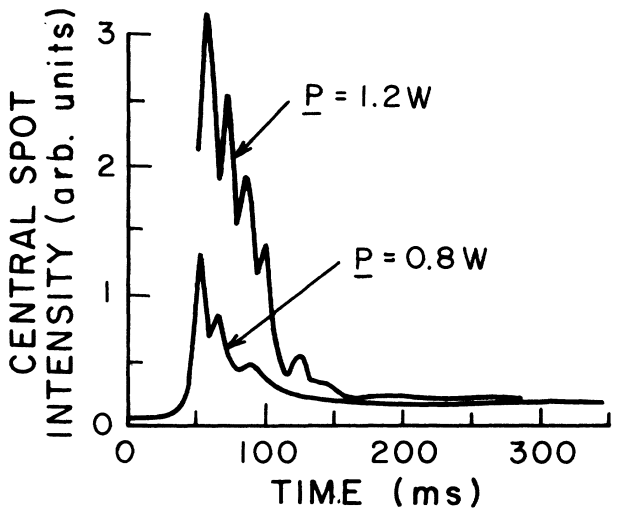

FIG. 9. Nonlinear transients in central spot intensity vs time at $P \approx 1$ W.

At powers $P \geq 1$ W the time dependence of the light scattered out from the central transmitted beam becomes nonmonotonic; transient pulses are observed, as shown in Fig. 9. Such pulses were also reported in Ref. 1 for fluids, but only at the lowest powers used, rather than the highest, as in our case. The oscillatory behavior shown in Fig. 9 may arise from nonlinear diffusion.

IV. DISCUSSION

We have considered other possible mechanisms for the phenomena discussed. In particular, we know that two-wave and four-wave coherent mixing occur in this material.[11] In the two-wave mixing scheme encountered in phase conjugation experiments, there is a forced optic diffusion of charged defects to accumulate at nodes in the standing waves produced by the incident laser. However, such an effect has never been observed at the high temperatures (800–850 K) used in our experiments, due to the very rapid thermal rediffusion of such charged defects. In addition, the rise times and recovery times we observe are rather slow and suggest thermal effects. Also, the c polarization of both incident and scattered beams rules out birefringence-induced phase-matched coherent mixing. Most significant is the fact that for phase-matched scattering due to photorefractive mechanisms, the beam divergence angle θ is independent of power P, depending only upon birefringence, whereas in our experiments, as shown in Fig. 5, θ varies linearly with P. Finally, the widths of the rings we observe (Fig. 3) are rather broad, much wider than those observed in coherent mixing experiments.[12–14] In barium sodium niobate we find that dn_c/dT remains finite at T_c, corresponding to a minimum in $F_\infty(T)$ at T_c. It might be more interesting to measure dn_c/dT by the technique employed here in a system in which this derivative is thought to diverge.[4] In such a crystalline phase transition it might be possible to measure very accurate values of dn/dT near T_c, which would facilitate evaluation of critical exponents and fluctuation contributions. Barium sodium niobate is a very poor choice for such precise work, because of its highly elevated transition temperature. $BaMnF_4$ might be a better choice,[15] as would SbSI, $NaNO_5$, or $PbMn_xNb_{1-x}O_3$. Our studies of these materials are in progress.

V. HIGH-POWER PHENOMENA

If we increase laser power significantly above 1 W, a number of new phenomena are observed. As many as

twenty sharp, concentric elliptical rings are observed. They are similar to the patterns originally reported in fluids by Akhmanov and co-workers[16–18] and Dabby and co-workers[19,20] and are approximately higher-order Bessel functions that arise in the description of phase modulation effects in thermal focusing. We also see, in addition to the temporal pattern shown in Fig. 9, chirping of the transmitted signal, and we see a clear fourfold crystalline symmetry in the far-field pattern, due to the anisotropy of the thermal conductivity k_T along different crystal directions. (Note that k_T is rather isotropic at ambient temperatures[6] but apparently not so near T_c.)

ACKNOWLEDGMENTS

This work was supported in part by the U.S. Army Research Office (ARO) Grant No. DAAL-03-86-K-0053.

*Present address: Department of Physics, California Institute of Technology, Pasadena, CA.

†Permanent address: Department of Physics, University of Toledo, Toledo, OH.

[1]J. P. Gordon, R. C. C. Leite, R. S. Moore, S. P. S. Porto, and J. R. Whinnery, J. Appl. Phys. **36**, 3 (1965).

[2]Chemming Hu and J. R. Whinnery, Appl. Opt. **12**, 72 (1973).

[3]G. Gehring, Adv. Phys. **29**, 731 (1980); J. Appl. Phys. **53**, 8152 (1982); Rep. Prog. Phys. **47**, 513 (1984).

[4]D. A. Atkins, W. F. Oliver, and J. F. Scott, Bull. Am. Phys. Soc. **33**, 539 (1988).

[5]T. Yamada, H. Iwasaki, and N. Niizeki, J. Appl. Phys. **41**, 4141 (1970).

[6]G. H. Burkhart and R. R. Rice, J. Appl. Phys. **48**, 4817 (1977).

[7]J. E. Murray, R. J. Pressley, J. H. Boyden, and R. B. Webb, IEEE J. Quantum Electron. **QE-10**, 263 (1974).

[8]S. Singh, D. A. Draegert, and J. E. Geusic [Phys. Rev. B **2**, 2709 (1970)] give $dn_c/dT=+3\times10^{-4}$ K^{-1} a few degrees from T_c, but a value nearly five times larger very near T_c seems evident from Fig. 1 (Ref. 5).

[9]M. V. Klein and T. E. Furtak, *Optics* (Wiley, New York, 1986), pp. 236–240.

[10]S. J. Sheldon, L. V. Knight, and J. M. Thorne, Appl. Opt. **21**, 1663 (1982).

[11]J. F. Scott, Bull. Am. Phys. Soc. **32**, 706 (1987); W. F. Oliver and J. F. Scott, *Incommensurate Crystals, Liquid Crystals and Quasi-Crystals,* edited by J. F. Scott and N. A. Clark (Plenum, New York, 1987), p. 177.

[12]J. O. Feinberg and R. Hellwarth, Opt. Lett. **5**, 519 (1980); and in *Incommensurate Crystals, Liquid Crystals and Quasi-Crystals,* Ref. 11, pp. 381 and 399.

[13]S. Odoulov and M. Soskin, *Laser Optics of Condensed Matter,* edited by J. L. Birman, H. Z. Cummins, and A. P. Kaplyanskii (Plenum, New York, 1988), p. 391.

[14]R. A. Rupp and F. W. Drees, Appl. Phys. B **39**, 223 (1986).

[15]R. V. Pisarev, B. B. Krichevtzov, P. A. Markovian, O. Yu. Korshunov, and J. F. Scott, Phys. Rev. B **28**, 2677 (1983).

[16]S. A. Akhmanov, D. P. Krindach, A. P. Sukhorukov, and R. V. Khokhlov, Pis'ma Zh. Eksp. Teor. Fiz. **6**, 509 (1967) [JETP Lett. **6**, 38 (1967)].

[17]S. A. Akhmanov, D. P. Krindach, A. V. Migulin, A. P. Sukhorukov, and R. V. Khokhlov, IEEE J. Quantum Electron. **QE-4**, 568 (1968).

[18]S. A. Akhmanov, A. P. Sukhorukov, and R. V. Khokhlov, Zh. Eksp. Teor. Fiz. **50**, 1537 (1966) [Sov. Phys.—JETP **23**, 1025 (1966)]. It must be noted that the first observation of a positive thermal-lens effect in a ferroelectric crystal was by this group, who reported a ring pattern in $LiNbO_3$ at room temperature as a peripheral figure in their work on fluids. This observation was recently brought to our attention.

[19]F. W. Dabby, T. E. Gustafson, J. R. Whinnery, Y. Kohanzadeh, and P. L. Kelley, Appl. Phys. Lett. **16**, 362 (1970).

[20]J. R. Whinnery, D. T. Miller, and F. W. Dabby, IEEE J. Quantum Electron. **QE-3**, 382 (1967).